5-28-2011

# Time variant cross correlation to assess residence time of water and implication for hydraulics of a sink-rise karst system

V. Bailly-Comte

Jonathan B. Martin

E. J. Screaton

# Time variant cross correlation to assess residence time of water and implication for hydraulics of a sink-rise karst system

V. Bailly-Comte,[1,2] Jonathan B. Martin,[1] and E. J. Screaton[1]

Received 3 June 2010; revised 24 November 2010; accepted 12 January 2011; published 28 May 2011.

[1] Transport rates and residence time in the subsurface are critical parameters for understanding water-rock interactions for efficient contaminant remediation. This paper presents a methodology for assessing flow and transit time of water through hydrological systems, with specific applications to karst systems and implication for hydraulics of a conduit system surrounded by a porous and permeable intergranular matrix. A time variant cross-correlation function analysis is applied to bivariate time series that characterize mass transfer, assuming a stationary system using sliding windows of various sizes. We apply the method to 1 year long temperature records in the Santa Fe River (north central Florida) measured at (1) the River Sink, where all the incoming surface water drains into a sinkhole, (2) Sweetwater Lake, where the river resurges into a 500 m long karst window, and (3) the River Rise, where the water discharges from a first-magnitude karst spring. Results are compared with those obtained using specific conductivity. Estimated residence time ranges from less than 1 day during floods to more than 15 days during base flow within the 8000 m flow path between the River Sink and the River Rise. Results are used to characterize geometric, hydraulic, and hydrodynamic properties of this sink-rise system with strong matrix-conduit interactions. These properties are critical to the chemical and physical behavior of surface water–groundwater mixing. Our results also have direct implications for sampling strategies and hydrograph separation of many karst systems with different degrees and types of matrix porosity and permeability.

**Citation:** Bailly-Comte, V., J. B. Martin, and E. J. Screaton (2011), Time variant cross correlation to assess residence time of water and implication for hydraulics of a sink-rise karst system, *Water Resour. Res., 47*, W05547, doi:10.1029/2010WR009613.

## 1. Introduction

[2] Many chemical and physical parameters, including pH, turbidity, fluorescence, major ion concentrations, specific electrical conductivity (SpC), and temperature, can now be recorded accurately at high frequency in surface water and groundwater, providing numerous natural tracers for hydrogeological studies. Each tracer is likely to be affected differently by dispersion, chemical reaction, sediment transport, water exchange with surrounding rocks, or other physicochemical characteristics, and thus, each could provide unique information about transport and residence times. Temperature has been used for more than 60 years and still remains a widely used natural tracer of flow [*Anderson*, 2005]; only recently has technology been developed for high-resolution monitoring of many other parameters.

[3] Temperature in surface streams reflects atmospheric temperature and thus can exhibit diel and seasonal variations as well as intermediate time scale variations derived from mesoscale weather patterns. Extreme weather can lead to floods, which drive large and rapid changes in both temperature and chemical composition. The range in time scales for these processes results in short- to long-term frequencies in physical and chemical characteristics of water that are integrated at the scale of the recharge area. Although complex, this range of frequencies could be used to track the time required for water to travel from the recharge area to the discharge area. Temperature variations, in particular, have been used to identify surface water infiltration, flow through fractures, and flow patterns in groundwater basins, as reviewed by *Anderson* [2005].

[4] Numerous examples exist of the ways in which temperature has been used to track flow. For example, time series analyses of temperature have been used to estimate seepage from and into stream beds [*Stonestrom and Constantz*, 2004; *Hatch et al.*, 2006]. Measuring vertical temperature profiles in streambeds is a simple and useful indicator of flow directions between surface water and groundwater and is used to identify gaining and losing streams [*Winter et al.*, 1998; *Stonestrom and Constantz*, 2004]. Numerous studies [e.g., *Hatch et al.*, 2006] proposed methods based on Fourier transform of time series to estimate pore water velocity and streambed seepage in the hyporheic zone. These methods use diurnal properties of temperature signals in the frequency domain and are based on changes in the phase and amplitude of thermal waves that move from the stream into the streambed at a targeted

[1]Department of Geological Sciences, University of Florida, Gainesville, Florida, USA.
[2]Laboratoire HydroSciences Montpellier, UMR 5569, Université Montpellier 2, Montpellier, France.


0043-1397/11/2010WR009613

frequency of 1 day [*Hatch et al.*, 2006; *Keery et al.*, 2007]. These techniques provide accurate results when the delay is less than the targeted frequency, which is appropriate in hyporheic exchange. These techniques may not be appropriate for tracing groundwater flow where transit times of more than a day may occur since the phase lag only gives the delay modulo the wavelength of 1 day. For example, this technique will give the same result for a lag of 8, 32, or 56 h, etc., which is not a problem when the lag is obviously less than 1 day (hyporheic exchanges) but is useless when the lag is unknown and probably higher. Thus, to adapt these approaches to longer time frames, we develop here a time domain method using cross-correlation functions (CCF) at various time scales.

[5] Assessments of discharge and flow velocity have also used natural tracers in karst systems to infer geometric properties of karst conduits. *Martin and Dean* [1999] recommended the simultaneous use of two or more different natural tracers, such as temperature and electrical conductivity, to obtain additional information about the conduit system as compared to the analysis of only a single parameter. *Birk* [2002] supported this idea by the means of theoretical modeling of flow and mass transfer in an idealized karst drainage network. *Birk et al.* [2004] showed with field experiments that, in general, SpC is a better tracer for the determination of time lags and thus the resulting estimation of conduit volumes; however, SpC could not distinguish surface water and groundwater in their system because of similar values in the two source waters. Instead, temperature, especially the attenuation of daily patterns in the time series, provided better information about origin and mixing of surface water and groundwater than SpC.

[6] Previous time series analyses of natural tracers [*Birk et al.*, 2004; *Screaton et al.*, 2004] consist of tracking rapid changes of temperature from base flow to stormflow. Such analyses typically rely on only a few measurements and assume the observed rapid changes provide hydrodynamic information that can be extrapolated to other time periods and events. Rapid changes usually occur when flow is transient and thus may not represent the hydrodynamic behavior of the system at all conditions. Temperature records are often available during times of common hydrologic behavior, e.g., recession and base flow periods. These records typically have muted signals, and no quantitative method exists to extract estimates of flow velocity.

[7] Understanding hydrodynamics during all flow conditions is particularly important in karst regions, which are highly vulnerable to contamination because of the rapid transport of pollutants through conduits. Conduits form efficient drainage systems but often are difficult (or impossible) to explore and map. During floods, flow through conduits may recharge intergranular or fissured matrix porosity of the surrounding aquifer, driven by the head gradient between the matrix and the conduits within the aquifer [*Martin and Screaton*, 2001; *Martin et al.*, 2006; *Bailly-Comte et al.*, 2010]. This recharge mechanism provides an additional process, along with recharge into sinkholes or diffuse surface recharge, by which water supplies could be contaminated. Effective strategies for the management and protection of groundwater resources thus need to be based on reliable information about conduit systems in karst areas [*Birk et al.*, 2004] and need to consider the exchange of water between the conduits and matrix under various flow conditions. This information could be determined with time series analyses of high temporal resolution tracers such as temperature or SpC.

[8] Our paper presents a method to allow the interpretation of time series of temperature and SpC to characterize transport in surface water–groundwater systems under flood, recession, and base flow conditions. In contrast, an artificial tracer experiment only provides one estimate of mean tracer velocity, assuming steady state flow conditions.

[9] In section 2 a method is developed to apply time variant CCF analysis to flow velocity measurements. The method is applied to time series records in the Santa Fe River (north central Florida). Results from the Santa Fe River are used to evaluate the relative usefulness of temperature and SpC as natural tracers of flows in karst systems and to understand the geometric and hydraulic properties of the karst conduit system.

## 2. Method

### 2.1. Definition and Estimation of the Correlation Functions

[10] A biased estimate $C_{XY}(k)$ of the cross-covariance coefficient between the input and the output time series $(X, Y)$ of a physical system at lag $k$ is given by [*Box et al.*, 1994]

$$C_{XY}(k) = \begin{cases} \frac{1}{n}\sum_{t=1}^{n-k}(X_t-\bar{X})(Y_{t+k}-\bar{Y}), & k=0,+1,+2,\ldots,L, \\ \frac{1}{n}\sum_{t=1}^{n+k}(Y_t-\bar{Y})(X_{t-k}-\bar{X}), & k=0,-1,-2,\ldots,-L, \end{cases} \quad (1)$$

where $L$ is the truncation point [*Jenkins and Watts*, 1968]. The respective variances of $(X, Y)$ are given by the two autocovariance functions at lag 0 provided by substituting $Y$ for $X$ and $X$ for $Y$ in equation (1). Consequently, the standard deviations of $(X, Y)$ are $\sigma_{XX}=\sqrt{C_{XX}(0)}$ and $\sigma_{YY}=\sqrt{C_{YY}(0)}$, respectively. A biased estimate $R_{XY}$ of the cross-correlation function is given by [*Jenkins and Watts*, 1968]

$$R_{XY}(k)=\frac{C_{XY}(k)}{\sigma_{XX}\sigma_{YY}}, \; -L\le k\le L. \quad (2)$$

[11] Substituting $Y$ for $X$ and $X$ for $Y$ in equation (2) gives the two autocorrelation functions (ACF) $R_{XX}$ and $R_{YY}$.

### 2.2. A Tool for Characterizing Transfer Functions

[12] The CCF is a widely used analysis tool for transfer function identification of physical systems [*Box et al.*, 1994]. A theoretical linear time invariant system that best approximates a real process, for instance, a mass transfer from a recharge area to a spring, is completely specified by the covariance functions [*Jenkins and Watts*, 1968]. It can be shown that the cross-covariance function gives the impulse response of the system when the input time series is a pure random process, which is theoretically characterized by a zero ACF for all lags except 0.

[13] *Mangin* [1984] proposed a methodology based on the statistical properties of ACF and CCF to describe and

classify hydrodynamics of karst aquifers. *Mangin* [1984] used CCF analysis of rainfall and discharge relationships as an image of the impulse response of the karst system to recharge events, considering rainfall as a pure random process over one hydrological cycle. This stochastic approach has subsequently been applied at other time scales and to other relationships characterizing pressure or mass transfer, such as water level variation in wells [*Larocque et al.*, 1998; *Bailly-Comte et al.*, 2008], or time series representing mass transfer, such as SpC, temperature, or turbidity [*Larocque et al.*, 1998; *Bouchaou et al.*, 2002; *Massei et al.*, 2006].

[14] The link between the impulse response and the CCF has also been used to assess flow velocity with various applications. Among them, estimation of transit time is based on the property of the CCF that shows a maximum value when the time delay ($k$ in equation (2)) equals the flow transit time [*Beck et al.*, 1969]. The time delay $k$ can actually be used to compute the modal flow velocity since it approximates the time delay of the maximum of the impulse response. This flow velocity is, however, a good approximation of the mean flow velocity when heat diffusion and dispersion can be neglected in front of advection. In that case, the flow velocity is thus computed using the estimated time delay $k$ divided by the distance between the two sensors that give the input and output time series. The system that transforms the input time series into the output time series is considered as a delayed linear time variant system. The method consists of dividing the bivariate time series into sliding windows of a size such that the system may be considered as stationary on the time scale of the window length. Then, a peak-locating procedure in the CCF is used to estimate the time delay. For instance, *Thorne et al.* [1998] successfully measured current profiles using a CCF method based on measurement of suspended sediment during tides in an estuary. Such a method was also used at a much smaller scale in an ultrasonic flowmeter [e.g., *Sanderson and Yeung*, 2002]. Other applications are found in hydrometry, including two-dimensional CCF analysis for particle image velocimetry [*Creutin et al.*, 2003], blood flow measurement [e.g., *Sisbot*, 2005], and flow in a pipeline for industrial purposes [*Yang and Beck*, 1998].

[15] Time variant CCF computations using sliding windows are time domain analyses of time series that require numerous computation steps. The number of required steps can be minimized by using a predelay before computing the CCF [*Yang and Beck*, 1998]. A predelay is a rough estimate of the transit time that is applied to the input time series so that the time variant CCF analysis only considers a short range of lags ($k$ in equation (2)). As a result, the CCF computation will be centered on the predelay, which will limit the bias of the CCF estimates as well as the influence of other processes that may have a different response time, so the CCF estimate will better describe the cause and effect relationship between the input and output signals.

[16] The efficiency of a time variant CCF analysis is also directly related to the length of the sliding window. The length of the window should be chosen so that the isolated record is long enough to contain some variations in the input time series that are correlated to variations in the output time series, although long windows may invalidate the stationary assumption since the system response depends on the flow velocity in the conduits. In this study, spectral analysis is used to separate the different trends in the time series, which are then used to choose the length of the sliding windows.

## 2.3. Influence of Autocorrelated Time Series

[17] *Jenkins and Watts* [1968] show that autocorrelated processes that are theoretically not cross correlated nevertheless give good cross correlations. This is the main difficulty in CCF interpretation. For instance, *Eisenlohr et al.* [1997] used a statistical analysis of time series provided by a numerical model of a karst aquifer to show that climatic regime, especially the frequency of recharge events, influences estimates of CCF between rainfall (input) and spring discharge (output). This influence results from an invalid assumption that the input signal characterizes a random process, i.e., the input time series shows an ACF that remains high for increasing lags. Consequently, inferring information about the structure and the dynamics of a hydrological system using the CCF of autocorrelated time series may be misleading. The effect of strong ACF on transit time estimates has not been studied in great detail for industrial applications since the input signal is often chosen as white noise, which facilitates the interpretation of the CCF. However, when the input signal is autocorrelated, several investigators have proposed different confidence intervals for transit time estimates [*Beck*, 1981; *Beck and Plaskowski*, 1987; *Thorne et al.*, 1998]. These estimates of confidence interval are relatively complex and may be unreliable depending on how autocorrelated the input time series is compared to the system passband.

[18] To assess the influence of the ACF on the cross- correlation estimate, we assume that the mass transfer through the system can be described with a delay $d$ (pure advection) applied to the input time series $T_1$ and output time series $T_2$ and that both $T_1$ and $T_2$ can be described by a first-order autoregressive process, denoted AR(1), with parameters $\alpha_1$ and $\beta_1$, respectively, so that $0 < \alpha_1 < 1$ and $0 < \beta_1 < 1$. In this case, the autocorrelation function of $T_1$ is theoretically given by

$$R_{11}(k) = \frac{C_{11}(k)}{\sigma_{11}^2} = \alpha_1^{|k|}. \tag{3}$$

[19] The parameter $\alpha_1$ of the AR(1) process thus equals the autocorrelation coefficient for $k = 1$. Since the inertia of the system is a function of $\alpha_1$, larger $\alpha_1$ represent a greater memory effect, which means that two successive values are more dependent. Statistical relationships between ACF and CCF for a pure delayed system give

$$R_{12}(k) = \frac{h_0 \sigma_{11} \alpha_1^{|k-d|}}{\sigma_{22}}, \tag{4}$$

where $d$ is the delay and $h_0$ is the constant gain of the system. This allows expressing $|k\text{-}d|$ as a function of the CCF estimate $R_{12}(k)$:

$$|k - d| = \frac{1}{\ln(\alpha_1)} \left\{ \ln\left(\frac{\sigma_{22}}{\sigma_{11} h_0}\right) + \ln\left[R_{12}(k)\right] \right\}. \tag{5}$$

[20] The standard deviation of $R_{12}$ is used to obtain an estimate for the error in the CCF. *Jenkins and Watts* [1968] give the following expression for $\sigma_{R_{12}}$:

$$\sigma_{R_{12}(k)} = \sqrt{\frac{1}{n}\left(\frac{1+\alpha_1\beta_1}{1-\alpha_1\beta_1}\right)}. \quad (6)$$

[21] Differentiating equation (5) gives an estimate for the standard deviation of the time lag $k$:

$$\sigma_k = \left|\frac{\sigma_{R_{12(k)}}}{R_{12}(k)\ln(\alpha_1)}\right| = \frac{1}{n}\left|\frac{\left(\frac{1+\alpha_1\beta_1}{1-\alpha_1\beta_1}\right)}{R_{12}(k)\ln(\alpha_1)}\right|. \quad (7)$$

[22] Thus, as expected, the standard error $\sigma_k$ of the lag estimate decreases when the standard error of the cross correlation is low and the cross correlation is high and also when the parameters of the AR(1) processes increase. This relationship shows that the results will be less accurate if the AR(1) parameters are close to 1, whatever the value of the CCF estimate. This illustrates that the value of the cross correlation alone does not reflect the precision of the transit time estimate.

[23] As a result, the assessment of transit times using CCF analysis supposes that the real system may be approximated by a linear time invariant system for which the input time series shows low autocorrelation. In the case of mass transfer of a natural tracer, the linear assumption is justified if the main transport process is advection. The input time series requires low ACF, so the relationship between the input and output is clear. The low ACF may be obtained by prefiltering or differentiating the time series [*Jenkins and Watts*, 1968] so that white noise residuals of the input time series are obtained. Indeed, prewhitening the input time series consists of removing all forms of serial dependences (trend, cycles, and autoregressive components) to obtain white noise residuals. *Box et al.* [1994] showed that the CCF between a prewhitened input and a correspondingly transformed output is directly proportional to the impulse response function. Finally, the time invariant assumption should be verified by analyzing the transfer on successive small periods for which the system shows a relatively stationary behavior, or, in other words, for which a unique transfer function can produce the output time series by convolution with the input time series.

### 2.4. Implication for Physical Properties of a Karst Conduit System

[24] Groundwater in karst aquifers flows predominantly through conduits where water velocity can reach several meters per second during floods. Advection is the prominent mass transfer process, and time variant CCF analysis of natural tracers should thus be a suitable technique to assess flow velocity. We apply this technique to a karst conduit system in north central Florida, where focused recharge allows measurement of the input time series of natural tracers.

[25] The relationship between the estimated flow velocity and discharge can be used to assess the cross-sectional flow area and thus the hydraulic diameter of the conduit system [*Screaton et al.*, 2004]. In addition, some hydrodynamic parameters can be derived from the velocity field. For laminar groundwater flow through a homogeneous porous media, Darcy's law gives

$$U = Ki, \quad (8)$$

where $U$ (m s$^{-1}$) is Darcy velocity, or flux, $i$ (dimensionless) is the hydraulic gradient, and $K$ (m s$^{-1}$) is the hydraulic conductivity. For turbulent flow conditions in fully filled conduits, head losses are a function of the square of the flux. These so-called quadratic head losses are usually determined by the friction factor using the *Colebrook and White* [1937] or the *Nikuradse* [1950] equations, with the latter being more accurate in the case of fully rough flow, as expected in karst conduits [*Jeannin*, 1996]. We thus used the *Nikuradse* [1950] equation to characterize flow:

$$f = \frac{1}{\left(1.74 + 2\log_{10}\frac{r_h}{\varepsilon}\right)^2}, \quad (9)$$

where $r_h$ is the hydraulic radius, $\varepsilon$ is the wall roughness, and $f$ is the friction factor. Equation (9) can be rearranged using the hydraulic diameter $D_h = r_h/4$:

$$\frac{1}{\sqrt{f}} = -2\log_{10}\left(\frac{\varepsilon}{1.85D_h}\right). \quad (10)$$

[26] The friction factor is related to the flow velocity ($V$) and the hydraulic gradient ($i$) by the mean of the Darcy-Weisbach equation, where $g$ is the gravitational acceleration:

$$i = f\frac{V^2}{2gD_h}. \quad (11)$$

[27] Combining equations (10) and (11) gives

$$V = \left[-2\log_{10}\left(\frac{\varepsilon}{1.85D_h}\right)\sqrt{2gD_h}\right]\sqrt{i}. \quad (12)$$

[28] As a result, considering the conduit system as a rough pipe implies that the slope between the log of the hydraulic gradient and the log of the flow velocity is 0.5. The equation of the resulting line can be used to assess the relative roughness $\varepsilon/D_h$ and thus the friction factor when the hydraulic diameter is known. Conversely, the same plot will show a line of slope 1 for groundwater flows that follow equation (8). Depending on the flow conditions, known discharge, water levels, and flow velocities can be used to assess the equivalent hydraulic conductivity or the relative roughness of the drainage system.

## 3. Description of the Study Area

### 3.1. Geology and Hydrology

[29] The post-Cretaceous lithostratigraphy of the Florida platform is characterized by pre-Miocene carbonate-dominated rocks that constitute the Floridan aquifer system, locally covered by Miocene and younger siliciclastic-dominated rocks [*Miller*, 1990; *Martin and Dean*, 2001, and references therein]. Among the siliciclastic rocks, the

Hawthorn Group plays a prominent role in the hydrology; this group acts as an upper confining unit to the Floridan aquifer system but has been removed by erosion from much of west central Florida. The erosional edge, known as the Cody Scarp [*Brooks*, 1981], marks the boundary between the confined highlands (~50 m above sea level (asl)) to the east and the unconfined lowlands (~20 m asl) to the west (Figure 1; see the inset). All of the surface streams that cross the Cody Scarp become losing streams, and most of them sink completely into the highly karstified Floridan aquifer system.

[30] The Santa Fe River flows over 60 km from east to west before reaching numerous sinkholes at the eastern boundary of the Cody Scarp and ultimately sinking completely at the River Sink (Figure 1). Captured surface water flows underground through well-developed fully filled karst conduits, of which about 15 km have been mapped by cave divers (Old Bellamy Cave Project, 2005, http://cavesurvey.com/OldBellamy.HTM; hereinafter referred to as Old Bellamy Cave Project, 2005). The conduits are intersected by many karst windows before resurging at a first-magnitude karst spring at the River Rise (Figure 1). The River Sink has been connected to these karst windows, including Sweetwater Lake, and to the River Rise by *Hisert* [1994] using $SF_6$ as an artificial tracer. The length of this groundwater flow path between the River Sink and the River Rise is estimated to about 8000 m using the most recent available data from the Old Bellamy Cave Project (2005), with an intermediate length of about 5000 m between the River Sink and Sweetwater Lake.

### 3.2. Monitoring Network

[31] A monitoring network of wells and karst windows has been constructed around the sink-rise system to assess the exchange of water between the matrix and conduits [*Martin and Dean*, 2001; *Martin and Screaton*, 2001; *Screaton et al.*, 2004; *Martin et al.*, 2006; *Bailly-Comte et al.*, 2010]. River stage is recorded each day about 700 m upstream from the River Sink by the staff of the O'Leno State Park and is converted to discharge on the basis of a rating curve developed by the Suwannee River Water Management District (Figure 1, rating 3 for station 02321898). Eight wells have been screened close to the depth of the main conduit (17–30 m below ground surface), and four of these deep wells have an associated shallow well a few meters away that are screened across the water table (2–10 m below ground surface). Most wells are monitored for water level, conductivity, and temperature at a 10 min time interval. Among these wells, water level fluctuation in well 4 is considered to be representative of hydrodynamics of the carbonate matrix that surrounds the main conduit on the basis of times series analysis of the water level at the well and discharge at both the River Sink and the River Rise [*Moore et al.*, 2009; *Bailly-Comte et al.*, 2010]. Transmissivities have been estimated for the deep wells and show medium to relatively high values, ranging from 950 to 160,000 $m^2\ d^{-1}$ [*Martin et al.*, 2006]. Estimates of hydraulic conductivities using slug tests in both the deep and shallow wells are in the range of $10^{-3}$ to $10^{-5}$ m $s^{-1}$, with the shallow wells exhibiting about 1 order of magnitude higher values than the deep wells [*Langston*, 2009]. These results at a short spatial scale confirm that the Floridan karst aquifer is characterized by a matrix with nonnegligible hydraulic conductivities, although much lower than the equivalent hydraulic conductivity of the conduit system. This induces a clear dual-permeability behavior that is characterized by both short reaction time and long recession periods with sustained flows at the River Rise [*Bailly-Comte et al.*, 2010].

[32] Water level, temperature, and SpC are also measured at a 10 min time interval at the River Sink, in Sweetwater Lake, and a few hundred meters downstream from the River Rise (Figure 1), which is used to assess the discharge at the River Rise (Figure 1, station 02321910), applying the rating curve produced by *Screaton et al.* [2004].

### 3.3. Previous Studies Dealing With Time Series of a Natural Tracer

[33] The Santa Fe River sink-rise system is an ideal karst system to study the use of natural tracers such as temperature and SpC given the strong interactions between surface water and groundwater, as well as the good knowledge of the underground flow paths between the River Sink and the River Rise (e.g., Figure 1). *Martin and Dean* [1999] demonstrated that residence times of water in karst systems can be estimated by manually correlating maxima and minima from temperature records of recharged and discharged water and found that residence times of the water ranged from less than 1 day at high flow to more than 10 days at low flow. More recently, *Screaton et al.* [2004] successfully tracked the change of temperature between the River Sink, seven karst windows, and the River Rise during two relatively small flood events ($<20$ $m^3\ s^{-1}$). Transit time between the River Sink, the karst windows, and the River Rise was converted to flow velocity by considering a straight line distance between each point. Comparison with discharge at the River Rise showed that flow is reasonably represented as pipe flow with a cross-sectional area of 380 $m^2$. This value reduces to 290 $m^2$ if we consider a total length of 8000 m rather than the 6000 m assumed by *Screaton et al.* [2004], which gives an average diameter of 19 m for a single conduit. These results differ slightly from those reported by *Martin and Dean* [1999], who analyzed flows $>100$ $m^3\ s^{-1}$. Differences were assumed to be related to water losses from the conduit to the matrix during the flood [*Screaton et al.*, 2004].

## 4. Time Series Analysis

### 4.1. Time Domain Analysis

#### 4.1.1. Time Series Description

[34] Figure 2a shows the rainfall, discharge, temperature, and SpC from March 2008 to July 2009. Table 1 gives the main characteristics of these time series for the longest period for which data are available at the three monitored points (13 March 2008 to 9 March 2009), which approximately represents the 2008/2009 hydrological year.

[35] The main flood event (Tropical Storm Fay, Figure 2a) occurred in August 2008. This event is separated from other minor flood events in March 2008 and March to July 2009 by base flow conditions.

[36] Along with the discharge in the sink-rise system, temperature records at the River Sink, Sweetwater Lake, and the River Rise show variations through time that are similar to variations in the air temperature, but the amplitude of the variations are muted as water flows through the karst system.

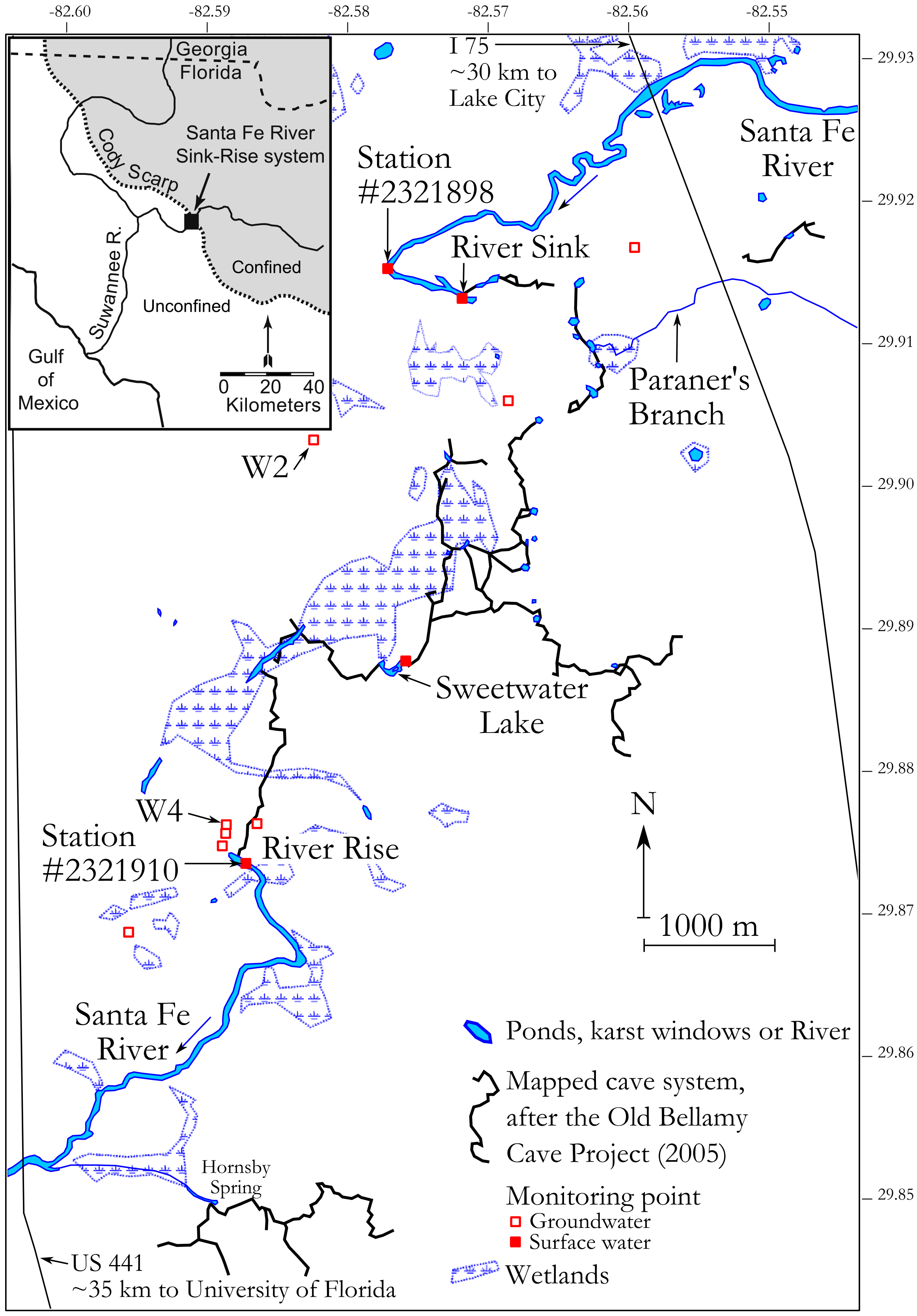
-82.60
-82.59
-82.58
-82.57
-82.56
-82.55
29.93
29.92
29.91
29.90
29.89
29.88
29.87
29.86
29.85
Georgia
Florida
Santa Fe River
Sink-Rise system
Cody Scarp
Suwannee R.
Confined
Unconfined
Gulf
of
Mexico
0 20 40
Kilometers
I 75
~30 km to
Lake City
Santa Fe
River
Station
#2321898
River Sink
Paraner's
Branch
W2
Sweetwater
Lake
N
1000 m
W4
Station
#2321910
River Rise
Santa Fe
River
Hornsby
Spring
US 441
~35 km to University of Florida
Ponds, karst windows or River
Mapped cave system,
after the Old Bellamy
Cave Project (2005)
Monitoring point
Groundwater
Surface water
Wetlands

**Figure 1**

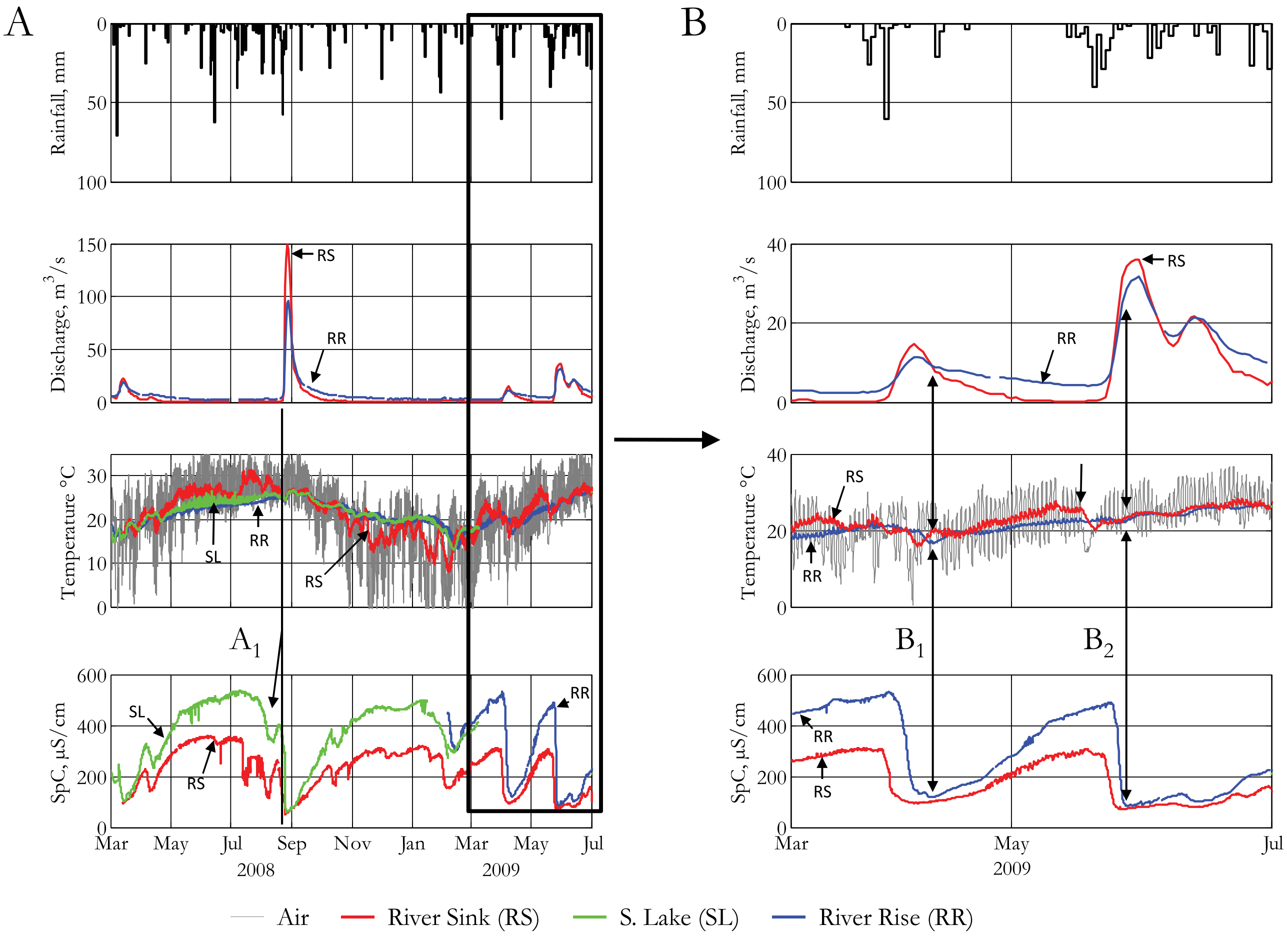


**Figure 2.** Time series recorded at the Santa Fe River sink-rise system (a) from March 2008 to July 2009 and (b) from March 2009 to July 2009. The rainfall is the daily average of the rainfall recorded at Oleno State Park (station 240) and at the 441 bridge (station 02321975, Santa Fe River at U.S. Route 441 near High Springs). The air temperature is measured 2 m above the ground ~12 km southeast of the site (station 260). Arrows and corresponding letters ($A_1$, $B_1$, and $B_2$) are used for references in the text.

This muting effect is also shown by the decrease of the standard deviation of the temperature downstream through the conduits (Table 1). The temperature time series clearly shows a lag during recession, and this lag is shorter during flooding. SpC values are similar at the three monitored points during flooding, with values less than 100 $\mu$S cm$^{-1}$, indicating that little groundwater, which has SpC values ranging from about 400 to 1300 $\mu$S cm$^{-1}$ [*Moore et al.*, 2009], mixes with the flood water as it passes through the karst system [e.g., *Martin and Dean*, 2001]. SpC values increase from the River Sink to the River Rise during recession and reach values higher than 500 $\mu$S cm$^{-1}$ at low flow, when groundwater provides most of the recharge. These high values result from mixing with groundwater from two sources [*Moore et al.*, 2009]: a diffuse recharge that equilibrates with calcite, as measured in well 4 (SpC = 430 $\mu$S cm$^{-1}$, $T = 21$°C), and another flow system characterized by dissolution and dedolomitization occurring deep within the aquifer [e.g., *Plummer*, 1977; *Hanshaw et al.*, 1979; *Jones et al.*, 1993], as measured in well 2 (Figure 1; SpC between about 700 and 1300 $\mu$S cm$^{-1}$ and $T = 26$°C).

[37] Each flood event exhibits a rapid decrease of temperature and SpC at the three monitored points, reflecting recharge of new event water with temperature and chemical compositions that are different from preevent water (Figure 2). Typically, discharge increases more rapidly at a karst spring following recharge events than the physical (temperature) and chemical (SpC) properties of the discharged water [*Birk et al.*, 2004]. The time lag between the pressure and mass transfer provides an estimate of the transit time of the infiltrating water through the conduit system [e.g., *Ashton*, 1966; *Atkinson*, 1977]. For instance, for the first flood event shown in Figure 2b (see $B_1$), the temperature and SpC minima at the River Rise occur after the maximum discharge, reflecting the delay between pressure and mass transfer. Temperature and SpC minima, however, occur at

**Figure 1.** Sketch map of the field area showing the locations of the Santa Fe River, its sink and rise, several intermediate karst windows, and the wells or karst features that are monitored. The mapped cave system has been drawn after the map of Old Bellamy Cave Project (2005). The numbers of the two gauging stations refer to the classification of the Suwannee River Water Management District.

**Table 1.** Main Statistical Characteristics of the Temperature and Specific Electrical Conductivity (SpC) Time Series Recorded at the Santa Fe River Sink-Rise System From March 2008 to March 2009[a]

| | Temperature (°C) | | | | SpC ($\mu$S cm$^{-1}$) | |
|---|---|---|---|---|---|---|
| | Air | River Sink | Sweetwater Lake | River Rise | River Sink | Sweetwater Lake |
| Mean | 20.1 | 21.4 | 21.7 | 21.4 | 244 | 381 |
| Standard deviation | 8.5 | 5.1 | 2.9 | 2.7 | 77 | 121 |
| Minimum | −6.5 | 7.9 | 13.0 | 13.4 | 50 | 61 |
| Maximum | 37.2 | 31.5 | 26.8 | 26.7 | 360 | 539 |

[a]The air temperature is measured 2 m above the ground elevation ∼12 km southeast of the site (station 260).

the River Rise before the maximum discharge during the second flood event (Figure 2b; see $B_2$). Furthermore, SpC shows strong fluctuations during the rainfall event for both the River Sink and Sweetwater Lake before the time of the flood peak in late August 2008 (see $A_1$ in Figure 2a). Since mass cannot be transferred before pressure, these variations result from local rainfall, which gives rise to a local but limited runoff that dilutes the water of the river, followed by flood water from the confined portion of the Santa Fe River watershed. Only runoff upstream from the River Sink produces high discharge in the River Rise, but both sources have similar effects on temperature and SpC time series. As a result, SpC and temperature cannot be used to characterize the flood peak transfer since they both characterize flood event water and local runoff at that time.

#### 4.1.2. Correlation Analysis

[38] ACF of SpC do not exhibit any periodic pattern, but ACF of both air and water temperature show daily periodic structures that are muted in water compared to the air (Figure 3). Diel variations are less pronounced at Sweetwater Lake than at the River Rise, but the amplitude at the River Rise is likely an artifact resulting from the placement of the sensor about 200 m downstream from the spring. Studying the transfer temperature at a target frequency of 1 day, as proposed for flows through the hyporheic zone [*Hatch et al.*, 2006; *Keery et al.*, 2007], may thus end up leading to erroneous conclusions about heat transfer in this sink-rise system.

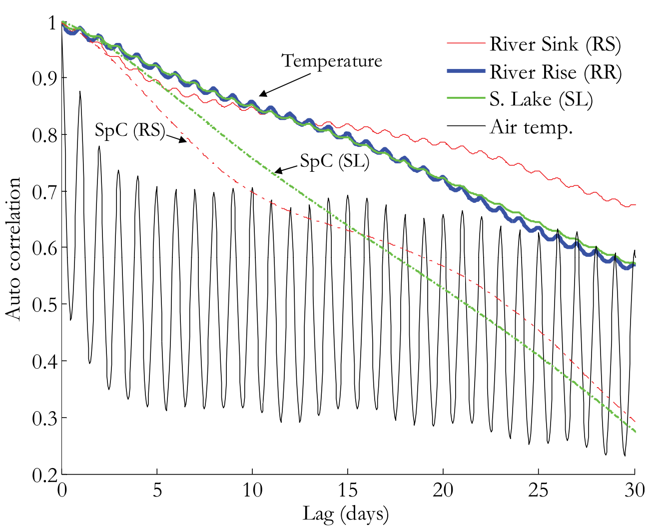


**Figure 3.** Autocorrelation functions (ACF) of hourly temperature and specific electrical conductivity (SpC) time series shown in Figure 2 over the longest period for which data are available (13 March 2008 to 9 March 2009), with an hourly time step.

[39] ACF of both temperature and SpC show strong autocorrelation coefficients (>0.85 and >0.7, respectively) for lags up to 10 days. These strong ACF will thus affect the CCF interpretation. Temperature shows two distinct ACF patterns depending on where the measurements were made. At the River Sink, the ACF for water and air temperature are similar, but the water has a higher correlation and smaller amplitude in its diel variation because of the memory effect of water resulting from the high heat capacity of water. Sweetwater Lake and the River Rise have ACF that are nearly identical to each other, but diverge from the ACF of the River Sink.

[40] Partial autocorrelation functions (PACF) have also been computed for two 1 month periods of flooding and recession (August–September 2008 and April–May 2009; see Figure 2) to determine if a window of width of 1 month can represent the flood and recession by an autoregressive process [*Box et al.*, 1994].

[41] Both temperature and SpC show a PACF value close to 1 at lag 1 but no correlation at a 95% confidence interval for others lags (Figure 4). Thus, both temperature and SpC time series can be described by an AR(1) process with an autoregressive coefficient of 1. This amounts to using a first differentiation filter before estimating the CCF.

### 4.2. Frequency Domain Analysis

[42] The discrete Fourier transform of autocovariance functions shows how amplitudes of each component giving rise to temperature and SpC time series are distributed over frequencies (Figure 5).

[43] Amplitude spectra of temperature time series decrease from upstream to downstream, and the highest amplitudes are in the air time series. This decrease shows that temperature variations are greater in the air than in the water, reflecting the high heat capacity of the water and that the karst system buffers the advective heat transfer from the River Sink to the River Rise, as reflected in the decrease in standard deviation in Table 1. The change of temperature spectra from the River Sink to Sweetwater Lake can be explained by a muted effect due to mixing with groundwater. Despite buffering, all temperature spectra are similar to each other, and thus heat transfer retained all of the time structure of the input signal, a characteristic of heat transfer with low dispersion. These spectra show low fluctuation for periods higher than approximately 30 days, which is denoted as the long-term frequency domain in the following discussion. For periods less than 10 days, the temperature

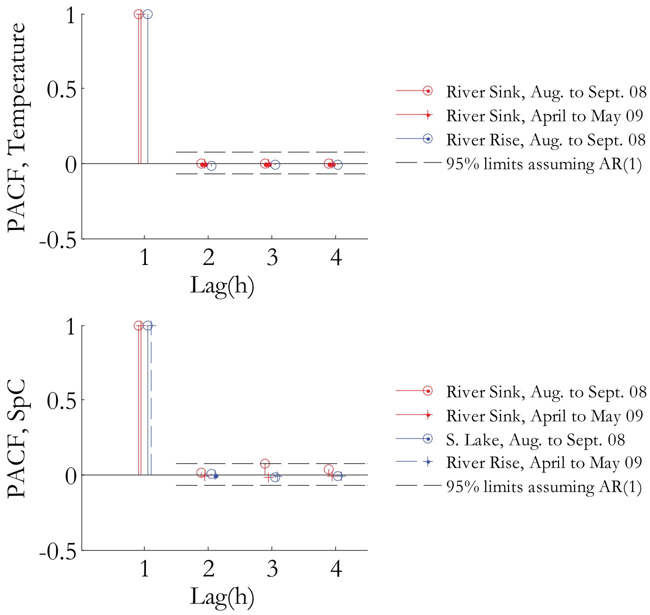


**Figure 4.** Partial autocorrelation function of the temperature and SpC time series estimated in Matlab® using the Levinson-Durbin recursions on the biased estimate of the ACF over two 1 month periods of flooding and recession (August–September 2008 and April–May 2009; see Figure 2). No temperature data are available at the River Rise for the second period.

spectra are variable with diurnal peaks with corresponding harmonics. These frequencies are denoted medium-term frequencies. High-frequency peaks depict harmonics that result from the representation of an asymmetrical air temperature record. Differences between the temperature spectra in the River Sink, Sweetwater Lake, and the River Rise become negligible and eventually reverse for higher frequencies. This effect illustrates that air temperature influences the water temperature, and consequently, the frequency domain less than approximately 6 h, denoted as short-term frequencies, should be considered cautiously before estimating the transit time.

[44] The SpC spectra are smoother and show higher values at Sweetwater Lake than at the River Sink, but there are too few records of SpC at the River Rise to confirm this evaluation (Figure 2a). Higher SpC spectra at Sweetwater Lake than the River Sink indicate that the SpC signal, unlike the temperature, is amplified by mixing with groundwater.

[45] Variance in SpC time series mainly originates from low-frequency fluctuations and from diel variations, probably related to in-stream biological and physicochemical processes such as temperature-related degassing of $CO_2$. The low-frequency domain gives rise to high ACF, and the transfer of the daily component of temperature is influenced by the air temperature, which means that these two frequency domains are not suitable for transit time estimates by CCF analyses. We thus propose to focus on the other frequency domains. Consequently, in this paper, we first use a long sliding window to roughly assess the transit time at a long time scale using a low-pass filter. Then, this estimate is used as a predelay to refine a subsequent time variant CCF analysis using a shorter sliding window and a high-pass filter to focus on medium term variations. The procedure is ultimately done at the shortest time scale given the resolution of the time series, using a first-order differential filter to remove the autocorrelation within the time series.

## 5. Time Variant CCF Analysis

### 5.1. Transit Time Between the River Sink and the River Rise

[46] We first consider various predelays, every 4 h from 2 to 8 days, and focus on the long-term transfer using only

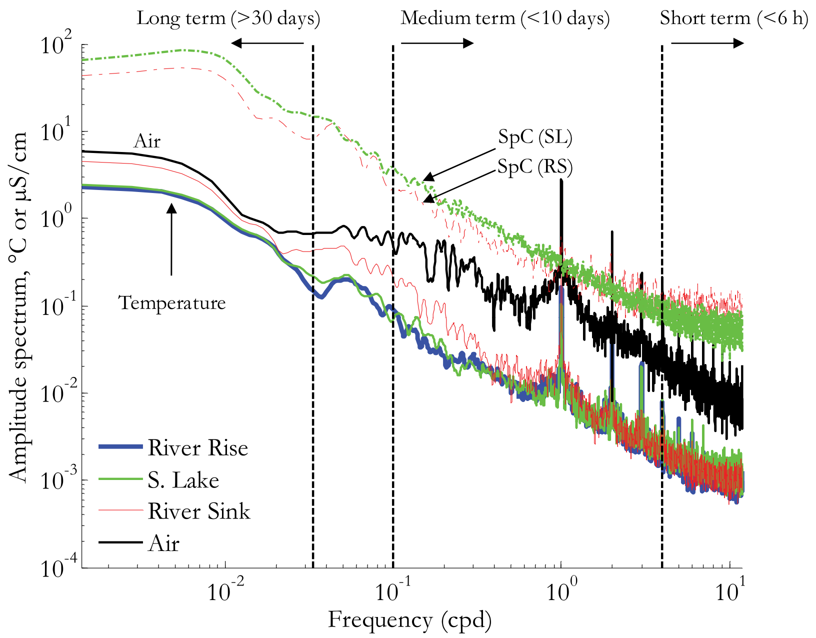


**Figure 5.** Amplitude spectra of temperature and SpC time series using ACF shown in Figure 3. Solid lines are used for temperature, and dashed lines are used for SpC.

(1) a large sliding window (30 days) and (2) prefiltered bivariate time series with a low-pass filter (Table 2). For each predelay, a peak locating procedure keeps only the lag for which the CCF is the highest. We also assume that the input-output time series describe an AR(1) process for a sliding window with a width of 1 month (Figure 4). Thus, we use equation (7) as a test for significance, rejecting CCF estimates with higher standard deviations than the sliding windows. Raw transit times are computed for each day, and the results are smoothed using a moving average of half of the window length.

[47] This long-term procedure gives a rough estimate of the transit time that is used as a predelay for the medium-term analysis described in Table 2. The main differences with the long-term procedure are that the prefiltering removes both the long-term (periods higher than 10 days) and the periodic structures at 1, 2, and 3 cycles per day (cpd) using a stop band filter (Table 2). In addition, the test of significance is directly based on the correlation coefficient since the high-pass filter removes the strong autocorrelation within the time series. We use a test of significance based on a 50% probability that the CCF does not describe the realization of a random process [*Jenkins and Watts*, 1968], which would indicate that the peak in the CCF has no meaning.

[48] The results of the medium-term procedure are ultimately used as a predelay for the short-term analysis that uses the differenced time series (Table 2). Thus, the short-term analysis uses results of both long- and medium-term analyses. The length of the window is 1 day for the short-term procedure, which is considered as a suitable time resolution for our study since only daily discharge is available.

[49] Results of the short-term analysis provide the best estimate of the transit time given the time resolution of the time series. Transit time variation is compared with the mean discharge of the River Sink and the River Rise computed for the period of time defined by the transit time, which is shown in Figure 6. Estimated residence time between the River Sink and the River Rise varies with the discharge and ranges from less than 1 day during flood to more than 15 days for base flow. Large variations of transit time occur during base flow and correspond to periods of high rainfall, which illustrates the limit of the method when local rainfall influences the transfer (Figure 6). In addition, low discharge particularly degrades the quality of the temperature because of the relative influence of air temperature. The recession periods are thus assumed to give a better estimate of the transit time than base flow; these periods are shown in Figure 6 by dots on the decreasing limbs of the hydrograph.

### 5.2. Comparison Between Temperature and SpC Time Series

[50] We also applied this procedure to temperature and SpC records between the River Sink and Sweetwater Lake (Figure 7). Transit times differ for temperature and SpC for the low-flow periods but are similar during flood and recession, supporting their utility during recession periods. During periods of drought, as exemplified by data from December 2008 to March 2009 (Figure 7), transit times estimated by SpC are lower than transit times estimated by temperature. Transit times from SpC are also lower than expected for low-flow conditions (especially in January 2009), which means that the method is relatively sensitive to the choice of the natural tracer (SpC or temperature) according to its statistical properties. Indeed, a natural tracer of water flow should reflect changes of water flow velocity according to time, which requires frequent variations in the time series of the natural tracer, so that correlation analysis is able to track the signal. Because of frequent and relatively random variations in temperature resulting from variations in air temperature, temperature is more suitable for hydrodynamics studies at low flow than SpC. These conclusions differ with those of *Birk et al.* [2004]. Chemical data, and thus SpC time series, may be more suitable for groundwater age characterization in other karst systems where only diffuse recharge occurs.

### 5.3. Advantages of the Statistical Analysis

[51] Although a less than 1 year long hourly time series, such as shown here, could have been analyzed with a deterministic approach, the main flood event recorded in August–September 2008 can be used to briefly illustrate the advantage of the statistical approach (Figure 8).

[52] The arrival of less mineralized flood water is clearly identified on the SpC time series in Sweetwater Lake, but the corresponding point is more difficult to detect at the River Sink. In addition, during the September recession (compare Figure 8 with Figure 2 showing discharge), variations of SpC are really attenuated, which makes SpC difficult to use as a natural tracer by a deterministic approach alone.

[53] For temperature, diel variations are observed at each monitored site most of the time. Use of temperature for transit time estimates is complicated when the time lag is longer than 1 day, as in September (see Figures 6 and 7). This complication is simplified deterministically by using long-term variations to detect which diel variations at the River Sink correspond to which diel variations at Sweetwater Lake or the River Rise. The statistical procedure

**Table 2.** Parameters of Time Variant CCF Procedure Applied to Temperature Time Series in the Santa Fe River Sink-Rise System Between March 2008 and July 2009

| | Step 1: Long Term | Step 2: Medium Term | Step 3: Short Term |
|---|---|---|---|
| Predelay | Every 4 h from 2 to 8 days | Moving average (window of 15 days) applied to long-term results | Moving average (window of 5 days) applied to medium-term results |
| Prefiltering | Low-pass filter, $fc = 1/30$ d$^{-1}$ | High-pass filter, $fc = 1/10$ d$^{-1}$ and stop band filters at $fc = 1, 2$, and 3 d$^{-1}$ | First-order differential filter |
| Length of the sliding window | 30 days | 10 days | 1 day |
| Test for significance | $\sigma_k < w$ (equation (7)) | 50% limits for $\sigma_{R_{12}}$ | 50% limits for $\sigma_{R_{12}}$ |

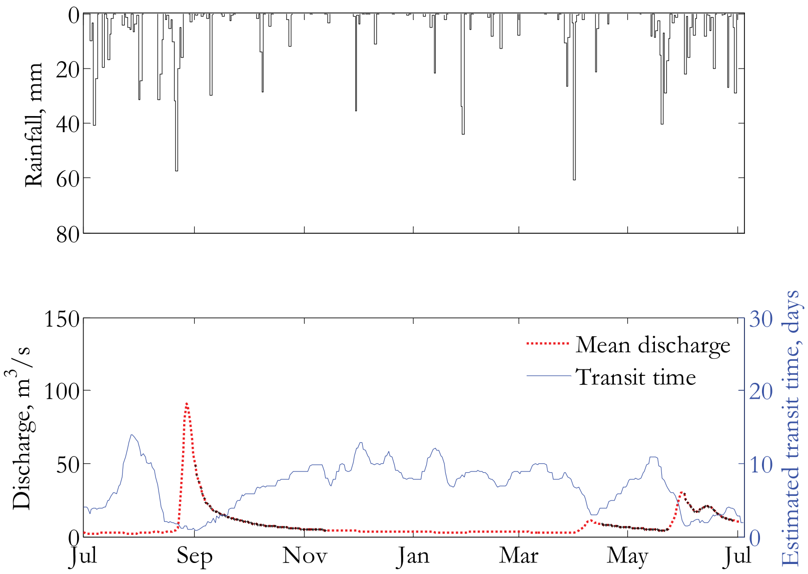


**Figure 6.** Results of the time variant CCF analysis using temperature time series showing the estimated transit time of the water that exits in the sink-rise system along with the mean discharge over the period of time defined by the transit time. The rainfall time series from Figure 2 shows the influence of local rainfall on this estimate. Dots on the hydrograph show the discharge–transit time couples during recession that are used in Figure 9.

described here effectively calculates the deterministic approach with the long- and medium-term analyses.

## 6. Implications for Geometric and Hydraulic Properties of the Karst Conduit System

### 6.1. Geometric Properties of the Conduit System

[54] Conduits have been mapped between the River Sink, Sweetwater Lake, and the River Rise, thereby allowing estimates of the mean flow velocity during the recession periods shown in Figure 6. The relationship between the estimated flow velocity and the mean discharge gives a straight line with a slope of 420 m$^2$ with a correlation coefficient $r^2 = 0.92$ (Figure 9). This slope also suggests that the conduit may have an average cross-sectional area of 420 m$^2$, or an average diameter of 23 m. The Peclet number is high ($>10^5$) over the entire period shown in Figure 6, which demonstrates that heat diffusion is negligible, even for low flow. In addition, the good linear relationship between flow velocity and discharge from the River Sink to the River Rise indicates that the time variant CCF analysis allows estimation of the velocity of the advective heat front. Thus, heat transfer

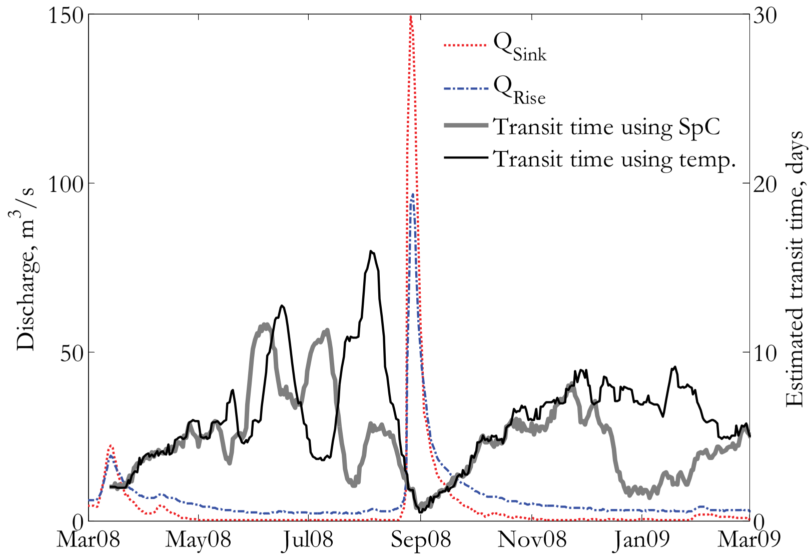


**Figure 7.** Comparison of the time variant CCF analysis provided by temperature and SpC time series at Sweetwater Lake from March 2008 to March 2009 along with the discharge measured at the River Sink and the River Rise.

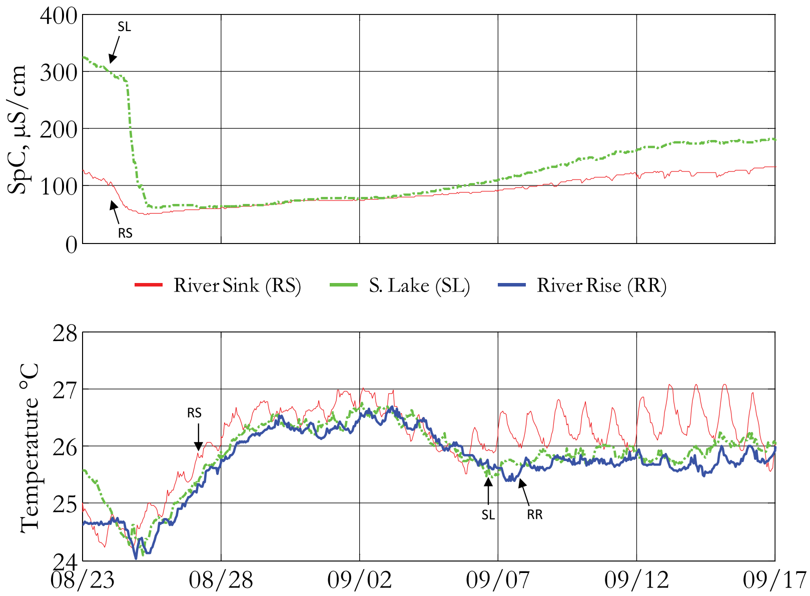


**Figure 8.** SpC and temperature time series at the River Sink, the River Rise, and Sweetwater Lake during a major flood event and its recession.

through the conduit system can be represented as equivalent to water movement in a single pipe for which advection is the main process. All these results are validated by numerous observations of cave divers (http://divefloridacaves.com/Santa Fe Underground.html) and previous work by *Screaton et al.* [2004] and *Martin and Dean* [2001].

[55] *Screaton et al.* [2004] found flow velocity slightly higher than our results for similar discharge (Figure 9), which can be explained since these authors based their estimation on the propagation of rapid change of temperature during the transfer of the flood peak only (see section 4.1).

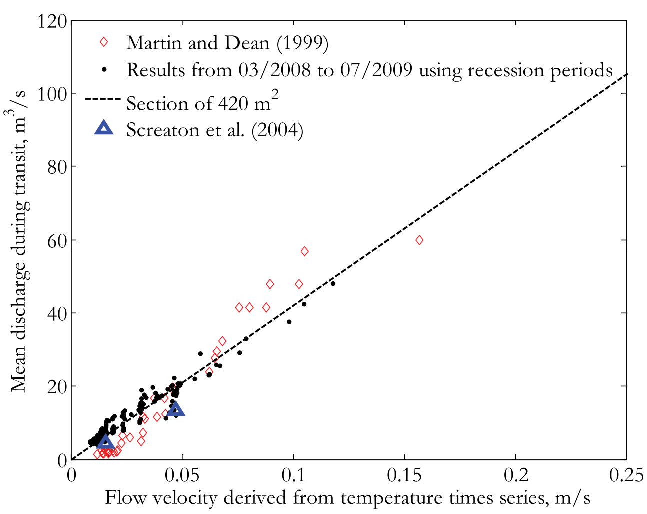


**Figure 9.** Relationship between estimated flow velocity by time variant CCF analysis of temperature time series and the estimated discharge in the conduit system using the recession periods shown in Figure 6. Results of previous studies, which may utilize different methods, are given for comparison. The dashed line represents a single theoretical conduit of 420 m$^2$ that does not exchange water with the matrix.

*Martin and Dean* [2001] found velocities less than our estimates of discharge during low flow and velocities higher than our estimates at high discharge; nonetheless, their results are close to the line defined by a cross-sectional area of 420 m$^2$. *Martin and Dean* [2001] based their estimates on the only available discharge data at the time, which was for the River Sink. Discharge should be higher at the River Rise than at the River Sink during low flow when the conduit gains water and lower during high discharge when the conduit loses water, resulting in an overestimation or underestimation of the discharge in the whole conduit system. Because our results are based on the mean discharge of the River Sink and the River Rise, there should be little overestimation or underestimation from the temperature, and thus there should be a better fit to a straight line.

[56] Using a similar approach as that used between the River Sink and the River Rise, we estimate the cross-sectional area of conduits between the River Sink and Sweetwater Lake to be about 486 m$^2$ ($r^2 = 0.94$), or a diameter of about 25 m. The conduit network is more complex between the River Sink and Sweetwater Lake than between Sweetwater Lake and the River Rise (Figure 1; see also http://divefloridacaves.com/Santa Fe Underground.html), and thus, flow could follow several conduits with a total area estimated from the transit times.

### 6.2. Hydraulic Properties of the Conduit System

#### 6.2.1. Results

[57] Hydrographs at the River Sink and the River Rise (Figure 2) reveal that part of the recharge from the River Sink is stored during a flood and slowly drains during the flood recession, as shown previously [*Martin and Dean*, 1999, 2001; *Martin and Screaton*, 2001; *Screaton et al.*, 2004; *Martin et al.*, 2006; *Bailly-Comte et al.*, 2010]. Our estimates of conduit size neglect the effect of water exchange between the conduit system and the matrix. Exchange is shown by inversion of the hydraulic gradient between the matrix and conduit [*Martin et al.*, 2006;

*Bailly-Comte et al.*, 2010] and differences in discharge measured at the River Sink and the River Rise compared to differences in water level at the River Rise and the matrix (well 4, Figure 10).

[58] Water levels that are lower in the matrix than in the conduit system (the River Rise) are denoted as a losing conduit in Figure 10. Conversely, periods when the conduit gains water begin as soon as the water level in well 4 is higher than the water level in the River Rise. Variations in water levels at the River Sink and the River Rise during a flood event and its recession are used to compute the hydraulic gradient $i$ within the conduit system, which means that the velocity head is neglected for the estimation of $i$. The velocity head is at most 2 mm for a flow velocity of 0.2 m $s^{-1}$ in the conduit system (Figure 9) and is thus minor relative to the observed head differences during high-flow events (Figure 10). In addition, during base flow, flow velocities and thus velocity heads are similar at the River Sink and the River Rise; thus, the error estimated by neglecting velocity head for the estimation of $i$ is compensated since the hydraulic gradient uses the difference of water level at the River Sink and the River Rise. As a result, the velocity head can be neglected in this study whatever the flow conditions given the size of the conduit system and the cross section of the Santa Fe River where water levels are measured.

[59] The relationship between the gradient and the flow velocity at the River Rise results in a hysteresis loop (Figure 11), which means that the discharge is not a simple function of the hydraulic gradient within the conduit system.

[60] During the initial part of the recession, the relationship between $i$ and the discharge has a slope of 1 while the conduit continues to lose water to the matrix. This portion of the recession shows a linear relationship between the hydraulic gradient and the discharge similar to laminar flows through porous media, reflecting an equivalent hydraulic conductivity $K = 1200$ m $s^{-1}$. This extremely high value has no physical meaning; it is a combination of the infinitely high hydraulic conductivity of an idealized but pressurized conduit system restrained by the hydraulic conductivity of the intergranular matrix.

[61] Then, during the second part of the recession, when the conduit system drains the matrix, the relationship between discharge and hydraulic gradient is also linear but has a slope of 0.5, which would be expected for a flow through a rough pipe (equation (12)). Considering a single conduit of 23 m diameter between the River Sink and the River Rise, the Reynolds number (*Re*) is between $10^5$ and $10^6$ for the period shown in Figure 10. This range is high enough to neglect *Re* on the friction factor estimate [*Nikuradse*, 1950], defining the fully rough flow condition (equation (9)). Combining equations (9) and (12) and the graphical adjustment on Figure 11 gives a relative roughness $\varepsilon/D_h = 1.0$ and a friction factor $f = 3.43$ (Figure 11).

[62] During the initial stages of a flood, when the hydraulic gradient quickly increases within the conduit system, the flow field between the conduit and the matrix is not in equilibrium. This disequilibrium gives rise to complex relationships between discharge and hydraulic heads that differ from the relationships during the recession. These disequilibrium conditions are difficult to describe (Figure 11; see the arrow marked "Flood").

### 6.2.2. Application to a Hydraulic Model of the Sink-Rise System

[63] The use of the linear law ($K = 1200$ m $s^{-1}$, equation (8)) and the quadratic law ($f = 3.43$, equation (12)) allows assessment of the discharge at the River Rise under these two assumptions using only variations in water level at the

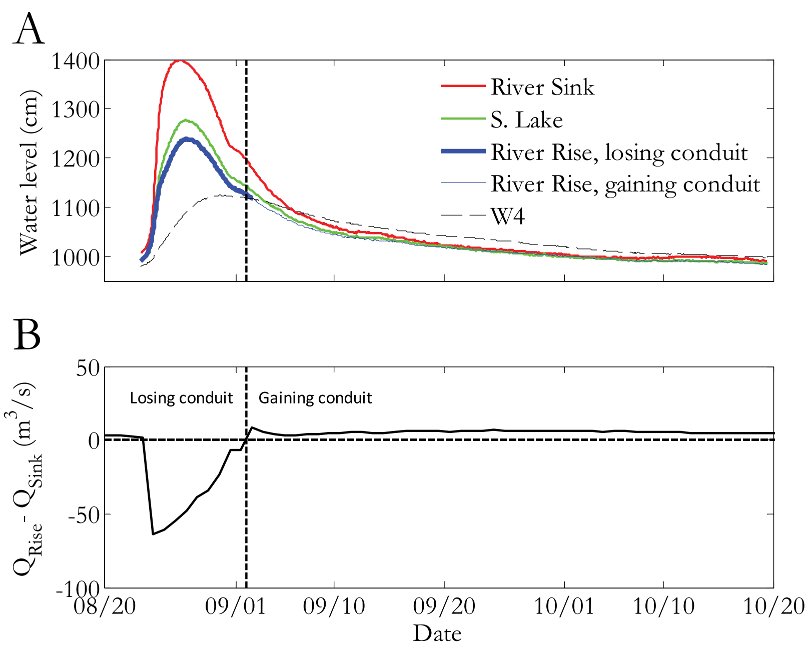


**Figure 10.** (a) Water level measured in the conduit system and in a well that represents the carbonate matrix (well 4) during the Fay event and its recession, showing the inversion of the hydraulic gradient between conduit and matrix systems [*Bailly-Comte et al.*, 2010]. (b) Variation in the difference of discharge measured at the River Rise and the River Sink.

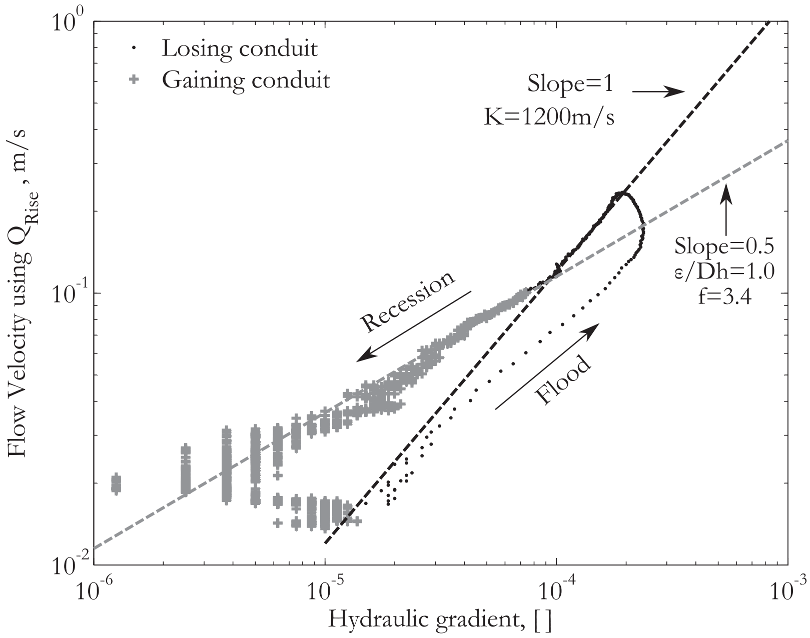


**Figure 11.** Relationship between the flow velocity derived from the hourly discharge measurements at the River Rise assuming a cross-sectional area of 420 $m^2$ and the hydraulic gradient between the River Sink and the River Rise on a logarithmic scale for the period shown in Figure 10. Straight lines with slopes of 1 and 0.5 closely fit the curve during recession as the conduit system is losing and gaining water, respectively.

River Rise and the River Sink. Figure 11 shows that the decreasing limb of the hydrograph at the River Rise is fit alternately by either the linear law or the quadratic law; specifically, during the recession, the linear model applies when the conduit is losing water, while the quadratic model applies when the conduit is gaining water.

### 6.2.3. Interpretation and Discussion

[64] The difference in discharge time series between the River Rise and the River Sink (Figure 10) shows that the flow of water from the conduit and the matrix is fast, while the release of water from the matrix to the conduits is slow and occurs over the entire recession period. The contrast in permeability between the conduits and the matrix is lower in this system than other karst systems and thus might not limit the exchange of water during floods as is usually observed in karst aquifers with low matrix porosity [*Bakalowicz*, 2005]. The use of the Darcy-Weisbach equation yields a lower discharge at the River Rise than the actual discharge at the beginning of the recession (Figure 12). The low estimated discharge suggests that the discharge capacity of the conduit system is exceeded [*Bonacci*, 2001; *Bailly-Comte et al.*, 2009] and some flood water flows through the matrix toward the River Rise in high-permeability zones within the matrix rocks. This condition occurs for discharge approximately higher than 50 $m^3\ s^{-1}$ but ultimately would contribute to discharge at the River Rise. Consequently, the conduit system restrains the flow rate according to its geometric and hydraulic properties, while variations in discharge result from groundwater flow variations through the matrix subsystem where equation (8) applies. The linear relationship between discharge and the hydraulic head better fits the observation in the losing conduit segment during the flood recession (Figure 12). This interpretation could be investigated further using a hydraulic numerical model, but it is consistent with the proposal that flow occurs through a halo of less consolidated matrix rock around the main conduits resulting from dissolution processes [*Moore et al.*, 2010].

[65] For the second part of the recession, once the conduit begins to gain, Figure 11 gives a relative roughness $\varepsilon/D_h$ of 1.0 for a diameter of 23 m. At this time, the conduit can drain both the matrix porosity and surface water coming from the River Sink. As a result, flow through the sink-rise system is mostly driven by hydraulic properties of the conduit system, following equation (12). Given the estimated diameter of the conduits, the absolute roughness $\varepsilon$ is approximately 23 m and should represent the average height of asperities inside the conduit. This extremely high value suggests that there may be numerous conduit constrictions and collapses, as proposed by *Atkinson* [1977] for even higher relative roughness ($\varepsilon/D_h$ close to 3) using *Colebrook and White*'s [1937] equation. Evidence for collapse is shown by the numerous karst windows that intersect the conduits between the River Sink and the River Rise (Figure 1). Alternatively, the high roughness we estimate could reflect the complex flow system between the River Sink and Sweetwater Lake (Figure 1).

[66] Figure 12 also shows that both models apply when the conduit system is neither losing nor gaining water around the first of September 2008. This means that the system is alternatively, but continuously, restrained by the hydrodynamic properties of the conduit and matrix subsystems, which shows that two reservoirs connected in parallel characterize the dual behavior of this karst aquifer. This observation has important consequences for conceptual models of karst springs since the transfer function in the phreatic zone should reflect hydrodynamic interactions between two reservoirs of different hydraulic conductivities and porosities.

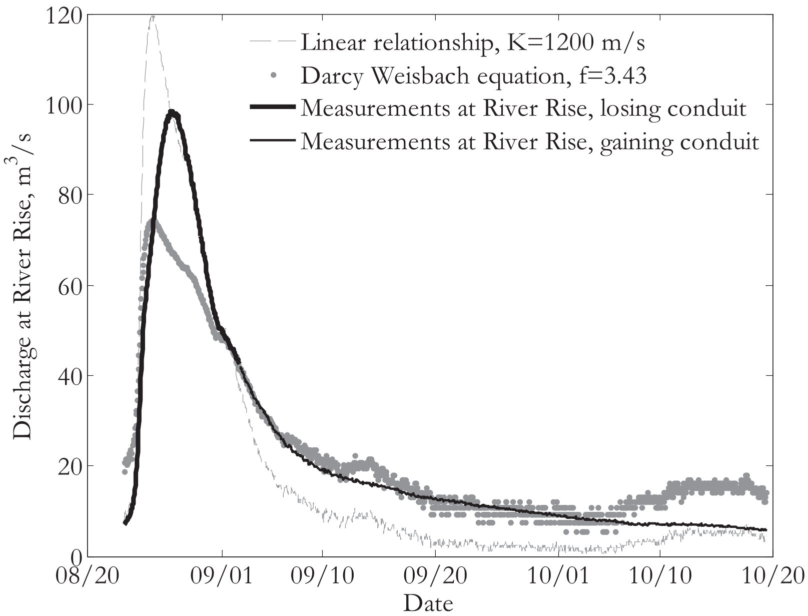


**Figure 12.** Comparison between the discharge at the River Rise and two computed discharge time series in the conduit system using water level measurements, assuming the application of a linear relationship and the Darcy-Weisbach equation. See text for discussion of relevance of a losing or gaining conduit for the computed discharge time series.

## 7. Summary and Conclusion

[67] We develop a time variant CCF method for determining transit time using time series of SpC and temperature and apply it to the Santa Fe River sink-rise karst system on the basis of the recognition that natural temperature or SpC variations in the allogenic stream propagate downstream through the conduits. This paper also shows that the use of rapid change of temperature or SpC during the transfer of the flood peak may be misleading because it may be strongly influenced by local runoff that precedes the flood peak transfer. Consequently, our statistical approach shows many advantages compared to a time-consuming manual procedure, and it could easily be applied to others sites where long time series of a natural tracer exist. At our site, temperature gives better results than SpC when only dynamics of flow is being estimated, especially during low flow because of frequent and relatively random variations in temperature that can be tracked by a CCF analysis, while information carried by SpC time series becomes poor because of mixing with groundwater. This time variant CCF analysis facilitates the use of time series of natural tracers and improves the understanding of the complex spatial and temporal dynamics of surface water–groundwater interactions. It has direct application to contaminant risk assessment, particularly for issues related to the spread of contaminants between surface and groundwater bodies.

[68] Flow velocities estimated from the CCF analysis allow the assessment of geometric and hydraulic properties of the conduit system between the River Sink and the River Rise. Flow is reasonably represented by a single pipe of 23 m diameter. Using this dimension and discharge and water level time series, we found that the drainage capacity of the conduit system is not sufficient for large flood events, forcing water to flow around the main conduit as "subconduit" flows. Such interaction would be comparable to hyporheic flows in streams. Consequently, hydrodynamic interactions between conduits and the matrix are key elements for understanding hydraulic and hydrodynamic behaviors of karst conduit systems, especially when matrix porosity and permeability are high.

[69] Our results will have direct implications for sampling strategies and hydrograph separation. The relationship between flow velocity and discharge can be used to better constrain a mixing model between surface water and groundwater at the River Rise that accounts for transit time in the karst system.

[70] **Acknowledgments.** The authors would like to thank the Florida Department of Environmental Protection and the staff of O'Leno State Park for their cooperation. We also would like to thank all the work accomplished by cave divers from the Old Bellamy Cave project. Santa Fe sink-rise research was funded by the National Science Foundation grants EAR-0853956 and EAR-0510054 and by the Florida Department of Environmental Protection grants S00060, S0141, and S0181.

## References

Anderson, M. P. (2005) Heat as a ground water tracer, *Ground Water*, *43*(6), 951–968.

Ashton, K. (1966), The analysis of flow data from karst drainage systems, *Trans. Cave Res, Group G. B.*, *7*, 161–203.

Atkinson, T. C. (1977) Diffuse flow and conduit flow in limestone terrain in the Mendip Hills, Somerset (Great Britain), *J. Hydrol.*, *35*, 93–110.

Bailly-Comte, V., H. Jourde, A. Roesch, S. Pistre, and C. Batiot-Guilhe (2008), Time series analyses for karst/river interactions assessment: Case of the Coulazou River (southern France), *J. Hydrol.*, *349*(1-2), 98–114.

Bailly-Comte, V., H. Jourde, and S. Pistre (2009), Conceptualization and classification of groundwater-surface water hydrodynamic interactions in karst watersheds: Case of the karst watershed of the Coulazou River (southern France), *J. Hydrol.*, *376*(3-4), 456–462.

Bailly-Comte, V., J. B. Martin, H. Jourde, E. J. Screaton, S. Pistre, and A. Langston (2010), Water exchange and pressure transfer between conduits

and matrix and their influence on hydrodynamics of two karst aquifers with sinking streams, *J. Hydrol.*, *386*(1-4), 55–66.
Bakalowicz, M. (2005), Karst groundwater: A challenge for new resources, *Hydrogeol. J.*, *13*(1), 148–160.
Beck, M. S. (1981), Correlation in instruments: Cross correlation flowmeters, *J. Phys. E Sci. Instrum. 14*(1), 7, doi:10.1088/0022-3735/14/1/001.
Beck, M. S., and A. Plaskowski (1987), *Cross-Correlation Flowmeters—Their Design and Application*, chapter 5, 240 pp., Adam Hilger, Bristol, U. K.
Beck, M. S., J. Drane, A. Plaskowski, and N. Wainwright (1969), Particle velocity and mass flow measurement in pneumatic conveyors, *Powder Technol.*, *2*(5), 269–277.
Birk, S. (2002), Characterisation of karst systems by simulating aquifer genesis and spring responses: Model development and application to gypsum karst, *Tübinger Geowiss. Arb. C60*, Universität Tubingen, Tübingen, Germany. (Available at http://w210.ub.uni-tuebingen.de/dbt/volltexte/2002/558)
Birk, S., R. Liedl, and M. Sauter (2004), Identification of localised recharge and conduit flow by combined analysis of hydraulic and physico-chemical spring responses (Urenbrunnen, SW-Germany), *J. Hydrol.*, *286*(1-4), 179–193.
Bonacci, O. (2001), Analysis of the maximum discharge of karst springs, *Hydrogeol. J.*, *9*(4), 328–338.
Bouchaou, L., A. Mangin, and P. Chauve (2002), Turbidity mechanism of water from a karstic spring: Example of the Ain Asserdoune spring (Beni Mellal Atlas, Morocco), *J. Hydrol.*, *265*(1-4), 34–42.
Box, G. E. P., G. M. Jenkins, and G. C. Reinsel (1994), *Time Series Analysis, Forecasting and Control*, 3rd ed., 598 pp., Prentice Hall, Englewood Cliffs, New Jersey.
Brooks, H. K. (1981), Physiographic divisions of Florida, Inst. of Food and Agric. Sci., Univ. of Fla., Gainesville.
Colebrook, C. F., and C. M. White (1937), Experiments with fluid friction in roughened pipes, *Proc. R. Soc. London, Ser A*, *161*(906), 367–381.
Creutin, J. D., M. Muste, A. A. Bradley, S. C. Kim, and A. Kruger (2003), River gauging using PIV techniques: A proof of concept experiment on the Iowa River, *J. Hydrol.*, *277*(3-4), 182–194.
Eisenlohr, L., M. Bouzelboudjen, L. Király, and Y. Rossier (1997), Numerical versus statistical modelling of natural response of a karst hydrogeological system, *J. Hydrol.*, *202*(1-4), 244–262.
Hanshaw, B. B., and W. Back (1979), Major Geochemical Processes in the Evolution of Carbonate-Aquifer Systems, in *Developments in Water Science*, edited by W. Back and D. A. Stephenson, pp. 287–312, Elsevier.
Hatch, C. E., A. T. Fisher, J. S. Revenaugh, J. Constantz, and C. Ruehl (2006), Quantifying surface water–groundwater interactions using time series analysis of streambed thermal records: Method development, *Water Resour. Res.*, *42*, W10410, doi:10.1029/2005WR004787.
Hisert, R. A. (1994), A multiple tracer approach to determine the ground and surface water relationships in the western Santa Fe River, Columbia County, Florida, PhD Thesis, University of Florida, Gainesville, Florida.
Jeannin, P.-Y. (1996), Structure et comportement hydraulique des aquifères karstiques, Ph.D. thesis, 237 pp., Univ. de Neuchâtel, Neuchâtel, Switzerland.
Jenkins, G. M., and D. G. Watts (1968), *Spectral Analyses and Its Applications*, 525 pp., Holden-Day, San Francisco, Calif.
Jones, I. C., H. L. Vacher, and D. A. Budd (1993), Transport of calcium, magnesium and $SO_4$ in the Floridan aquifer, west-central Florida: Implications to cementation rates, *J. Hydrol.*, *143*(3-4), 455–480.
Keery, J., A. Binley, N. Crook, and J. W. N. Smith (2007), Temporal and spatial variability of groundwater-surface water fluxes: Development and application of an analytical method using temperature time series, *J. Hydrol.*, *336*(1-2), 1–16.
Langston, A. L. (2009), The relationship between specific conductivity and flow paths in a karst aquifer, north-central Florida, M.Sc. thesis, Univ. of Fla., Gainesville.
Larocque, M., A. Mangin, M. Razack, and O. Banton (1998), Contribution of correlation and spectral analyses to the regional study of a large karst aquifer (Charente, France), *J. Hydrol.*, *205*(3-4), 217–231.
Mangin, A. (1984), Pour une meilleure connaissance des systemes hydrologiques a partir des analyses correlatoire et spectrale, *J. Hydrol.*, *67*(1-4), 25–43.
Martin, J. B., and R. W. Dean (1999), Temperature as a natural tracer of short residence times for groundwater in karst aquifer, in *Karst Modeling*, pp. 236–242, Karst Waters Inst., Charles Town, W. Va.
Martin, J. B., and R. W. Dean (2001), Exchange of water between conduits and matrix in the Floridan aquifer, *Chem. Geol.*, *179*(1-4), 145–165.
Martin, J. B., and E. Screaton (2001), Exchange of matrix and conduit water with examples from the Floridan aquifer, *U.S. Geol. Surv. Water Resour. Invest. Rep.*, *01-4011*, 38–44.
Martin, J. M., E. J. Screaton, and J. B. Martin (2006), Monitoring well responses to karst conduit head fluctuations: Implications for fluid exchange and matrix transmissivity in the Floridan aquifer, *Spec. Pap. Geol. Soc. Am.*, *404*, 209–217.
Massei, N., J. P. Dupont, B. J. Mahler, B. Laignel, M. Fournier, D. Valdes, and S. Ogier (2006), Investigating transport properties and turbidity dynamics of a karst aquifer using correlation, spectral, and wavelet analyses, *J. Hydrol.*, *329*(1-2), 244–257.
Miller, J. A. (1990), Ground water atlas of the United States, Alabama, Florida, Georgia and South Carolina, *U.S. Geol. Surv. Hydrol. Invest. Atlas, HA-730-G*.
Moore, P. J., J. B. Martin, and E. J. Screaton (2009), Geochemical and statistical evidence of recharge, mixing, and controls on spring discharge in an eogenetic karst aquifer, *J. Hydrol.*, *376*(3-4), 443–455.
Moore, P. J., J. B. Martin, E. J. Screaton, and P. S. Neuhoff (2010), Conduit enlargement in an eogenetic karst aquifer, *J. Hydrol.*, *393*(3-4), 143–155.
Nikuradse, J. (1950), Laws of flow in rough pipes, *Tech. Memo. 1292*, Natl. Advis. Comm. for Areonaut., Washington, D. C. (Available at http://ntrs.nasa.gov/archive/nasa/casi.ntrs.nasa.gov/19930093938_1993093938.pdf).
Plummer, L. N. (1977), Defining reactions and mass transfer in part of the Floridan aquifer, *Water Resour. Res.*, *13*(5), 801–812, doi:10.1029/WR013i005p00801.
Sanderson, M. L., and H. Yeung (2002), Guidelines for the use of ultrasonic non-invasive metering techniques, *Flow Meas. Instrum.*, *13*(4), 125–142.
Screaton, E., J. B. Martin, B. Ginn, and L. Smith (2004), Conduit properties and karstification in the unconfined Floridan aquifer, *Ground Water*, *42*(3), 338–346.
Sisbot, S. (2005), A cross-correlation technique as a system evaluation tool; application to blood flow measurement in extra-corporeal circuits, *Flow Meas. Instrum.*, *16*(1), 27–34.
Stonestrom, D. A., and J. Constantz (2004), Using temperature to study stream-groundwater exchange, *U.S. Geol. Surv. Fact Sheet, 2004-3010*.
Thorne, P. D., P. J. Hardcastle, and J. W. Dolby (1998), Investigation into the application of cross-correlation analysis on acoustic backscattered signals from suspended sediments to measure nearbed current profiles, *Cont. Shelf Res.*, *18*(6), 695–714.
Winter, T. C., W. H. Judson, O. L. Franke, and W. M. Alley (1998), Ground water and surface water a single resource, *U.S. Geol. Surv. Circ.*, *1139*.
Yang, W. Q., and M. S. Beck (1998), An intelligent cross correlator for pipeline flow velocity measurement, *Flow Meas. Instrum.*, *8*(2), 77–84.

V. Bailly-Comte, Laboratoire HydroSciences Montpellier, UMR 5569, Université Montpellier 2, F-34095 Montpellier, France. (bailly@msem.univ-montp2.fr)

J. B. Martin, E. J. Screaton, Department of Geological Sciences, University of Florida, 241 Williamson Hall, PO Box 112120, Gainesville, FL 32611, USA.